ELSEVIER

Remote Sensing of Environment 76 (2001) 360–372

Remote Sensing of Environment

www.elsevier.com/locate/rse

Directional effect on radiative surface temperature measurements over a semiarid grassland site

A. Chehbouni[a,*], Y. Nouvellon[b,1], Y.H. Kerr[a], M.S. Moran[b], C. Watts[c], L. Prevot[d], D.C. Goodrich[b], S. Rambal[e]

[a]*CESBIO (CNES-CNRS-IRD-UPS), 18 avenue Edouard Belin, 31401 Toulouse Cedex 4, France*
[b]*USDA-ARS-SWRC, Tucson, AZ, USA*
[c]*IMADES, Hermosillo, Sonora, Mexico*
[d]*INRA, Station de bioclimatologie, Avignon, France*
[e]*CNRS-CEFE, Montpellier, France*

Received 22 May 2000; accepted 9 December 2000

Abstract

In this study, an experimental design was conceived, as part of the Semi-Arid-Land-Surface-Atmosphere (SALSA) program, to document the effect of view angle variation on surface radiative temperature measurements. The results indicated differences between nadir and off-nadir radiative temperature of up to 5 K. The data also illustrated that, under clear sky and constant vegetation conditions, this difference is well correlated with surface soil moisture. However, the correlation decreased when the same comparison was made under changing vegetation conditions. To investigate the possibility of deriving component surface temperatures (soil and vegetation) using dual-angle observations of directional radiative temperature, two radiative transfer models (RTM) with different degrees of complexity were used. The results showed that despite their differences, the two models performed similarly in predicting the directional radiative temperature at a third angle. In contrast to other investigations, our study indicated that the impact of ignoring the cavity effect term is not very significant. However, omitting the contribution of the incoming long-wave radiation on measured directional radiance seemed to have a much larger impact. Finally, sensitivity analysis showed that an accuracy of better than 10% on the plant area index (PAI) was required for achieving a precision of 1 K for inverted vegetation temperature. An error of 1 K in measured directional radiative temperature can lead to an error of about 1 K in the soil and vegetation temperatures derived by inverting the RTM.

1. Introduction

Land surface temperature is a key variable for interpreting carbon, water and energy fluxes at the biosphere–atmosphere interface. Remote sensing of surface temperature has been successfully used to monitor temporal variability of surface fluxes across a wide range of spatial scales (e.g., Choudhury, Reginato, & Idso, 1986; Kustas et al., 1989; Moran, Humes, & Pinter, 1997; Moran et al., 1994; Taconet, Bernard, & Vidal-Madjar, 1986; Watts et al., 2000). However, Hall, Huemmrich, Goetz, Sellers, and Nickeson (1992) reported less successful results during the First International Satellite Land Surface Climatology Project (ISLSCP) Field Experiment (FIFE). The primary reason for such conflicting results is that remotely sensed surface temperature cannot be used to replace aerodynamic temperature in the heat flux equation. There are several approaches to take into account the difference between radiative and aerodynamic surface temperatures (Brutsaert & Sugita, 1996; Kubota & Sugita, 1994; Lhomme, Monteny, Troufleau, Chehbouni, & Bauduin, 1997; Stewart et al., 1994; Sugita & Brutsaert, 1996; Sun & Mahrt, 1995; Troufleau, Lhomme, Monteny, & Vidal, 1997; Zhan, Kustas, & Humes, 1996). Chehbouni, Watts, et al.

* Corresponding author. Tel.: +33-5-6155-8501; fax: +33-5-6155-8500.
E-mail address: ghani@cesbio.cnes.fr (A. Chehbouni).
[1] Present affiliation: CIRAD-Forêt, France.

0034-4257/01/$ – see front matter
PII: S0034-4257(00)00201-7

(2000) reported that the approach wherein an excess resistance is added to the aerodynamic resistance in the formulation of the sensible heat flux (Stewart et al., 1994) is functionally equivalent to the β approach of Chehbouni et al., (1996) and Chehbouni et al. (1997), which consists of directly modifying the difference between radiative and air temperatures. Both approaches need to be locally calibrated and are therefore difficult to apply a priori to different surface types. One possibility of avoiding such empirical approaches is through the use of the so-called dual source models where aerodynamic temperature is analytically computed in terms of the temperatures and resistances of soil, vegetation, and air (Blyth & Dolman, 1995; Lhomme et al., 1994; Shuttleworth & Wallace, 1985). However, the problem is that component surface temperatures (i.e., soil and vegetation) cannot be directly obtained from remote sensing measurements.

Several experimental studies have been dedicated to documenting directional effect on thermal infrared measurements over a wide range of surfaces (Caselles et al., 1992; Heilman et al., 1981; Jackson, Reginato, & Idso, 1977; Kimes 1980, 1981; Kustas et al., 1990; Mathias, et al. 1987; Sobrino & Caselles, 1990). Lagouarde et al. (2000) and Lagouarde et al. (1995) and presented a review of some of these experiments and documented the impact of changing view angle and sun angle geometry on radiative surface temperature measurements over different surfaces. In their papers, the need for correcting view angle effect on radiative surface temperature when using data from sensors with a pointing capability such as NOAA-AVHRR to infer surface fluxes was emphasized.

The feasibility of inferring component and structural information of the surface from multiple view-angle measurements of surface temperature was first investigated by Kimes (1983). During the past two decades, several models with varying degrees of complexity have been developed (e.g., Francois et al., 1997; Jackson et al., 1977; Kimes, 1983; Mathias et al., 1987; McGuire, et al. 1989; Prevot, 1985; Smith & Goltz, 1994). Interest in multidirectional thermal infrared measurements increased when data from the Along Track Scanning Radiometer (ATSR) instrument, aboard the first European Remote Sensing Satellite (ERS-1) became available (Prata, 1990). Still, there are few studies where multidirectional thermal infrared data have been used to derive surface fluxes over heterogeneous surfaces.

In this study, an experiment was designed to investigate the effect of view-angle variation on surface radiative temperature measurements over a semiarid grassland in Mexico during the Semi-Arid-Land-Surface-Atmosphere (SALSA) International Program (Chehbouni et al., 2000; Goodrich et al., 2000). The specific objectives of this study were: (1) to examine the directional effects on surface temperature measurements throughout the entire 1999 growing season with respect to changing vegetation conditions and soil moisture status; (2) to test the performance of two different models, with varying degree of complexity, for inverting soil and vegetation temperatures from dual-angle measurements of radiative surface temperature. The following sections provide a brief description of the two models used in this study: a description of the study site and the experimental setup, a discussion of the impact of changing surface conditions on the directional behavior of surface temperature, and a comparison of the performance and the robustness of the two models. The study concludes with an investigation of the relative sensitivity of the inversions to uncertainties in surface temperature measurements and surface characterization (soil and vegetation emissivity, vegetation characteristics such as the plant area index, PAI).

2. Modeling background

Following Lagouarde et al. (1995) and Norman and Becker (1995), for a natural surface, the spectral radiance $R_\lambda(\theta)$ observed by a radiometer in a direction θ, at a given wavelength λ, can be expressed as (Eq. (1)):

$$R_\lambda(\theta) = \varepsilon(\lambda,\theta)B_\lambda(T_r) + [1-\varepsilon(\lambda,\theta)]\mathrm{Ra}_\lambda, \quad (1)$$

where T_r is the directional radiative temperature of the surface; $B_\lambda(T_r)$ the Planck function; $\varepsilon(\lambda,\theta)$ the directional spectral emissivity, and Ra_λ the incoming long-wave radiation that reached the surface. The directional brightness temperature $T_b(\theta)$ is defined as the temperature of a black body that would emit the same radiance. An instrument with a spectral response $f(\lambda)$ in the band comprised between λ_1 and λ_2 leads to (Eq. (2)):

$$\int_{\lambda_2}^{\lambda_1} f(\lambda)B_\lambda[T_b(\theta)]\mathrm{d}\lambda = \int_{\lambda_2}^{\lambda_1} f(\lambda)R_\lambda(\theta)\mathrm{d}\lambda. \quad (2)$$

In the following, the waveband reference will be omitted since a nominal 8–14-μm band pass was considered. The directional emissivity and the directional radiative temperature result from contributions of different surface elements seen by the sensor. As in the visible and near-infrared bands, the relative contributions of individual surface elements to the total measurement depend on the view angle.

In this study, two radiative transfer models are used to infer component surface temperatures from observations at two angles. The first is a physically based model (hereafter called Mod1) developed by Kimes (1980) and improved by Prevot (1985). A complete description of Mod1 was presented by Francois et al. (1997) and Prevot (1985). Briefly, Mod1 is a probability model (turbid-medium model) that computes the directional canopy radiance as a function of sensor view angle, component temperatures and geometrical structure of the vegetation. The directional canopy radiance is obtained by summing the relative contributions of vegetation, ground and atmosphere layers. These contributions are calculated using the directional gap frequency (see below) through the vegetation. The vegetation is characterized by its PAI (the sum of leaf and stem area index), leaf and stem

inclination distribution function (LSIDF) and a dispersion parameter. An iterative procedure is used to compute the multiple reflections within the canopy and between the ground and the canopy. This model allows a detailed description of the temperature profile within the canopy, with the possibility of considering both shaded and illuminated soil and vegetation parts. However, for simplicity in this study, only mean soil and vegetation temperatures were considered. It should be noted that Mod1 explicitly takes into account the coupling between soil, vegetation and sky layers. Finally, the directional radiative temperature is expressed in terms of soil and vegetation temperatures and emissivities, directional gap frequency and incoming long-wave radiation.

The directional gap frequency depends on the canopy structure and foliage amount (PAI) in each vegetation layer, and can be expressed as (Eq. (3)):

$$b(\theta) = \exp\left[-\lambda(\theta)\frac{G(\theta)}{\cos\theta}\mathrm{PAI}\right], \tag{3}$$

where the ratio $G(\theta)/\cos\theta$ represents the directional extinction coefficient for a canopy with a random leaf dispersion, and $\lambda(\theta)$ is the directional leaf dispersion parameter which accounts for the departure from a canopy with a random leaf distribution (e.g., canopy clumping); $G(\theta)$ is the fraction of foliage projected in the direction θ, given by (Eq. (4)):

$$G(\theta_s) = \int_0^{\pi/2} A(\theta,\theta_l)g(\theta_l)\mathrm{d}\theta_l, \tag{4}$$

where $g(\theta_l)$ is the LSIDF (Campbell, 1986, 1990; Goel & Strebel, 1984), and $A(\theta,\theta_l)$ as the projection of unit leaf area with an inclination angle θ_l. $A(\theta,\theta_l)$ is given by Warren (1960) (Eqs. (5a) and (5b)),

$$\begin{cases} A(\theta,\theta_l) = \cos(\theta)\cos(\theta_l) & \text{if } \theta+\theta_l \le \pi/2 \\ A(\theta,\theta_l) = \cos(\theta)\cos(\theta_l)|2(\Phi_u - \tan(\Phi_u))/\pi - 1| & \text{if } \theta+\theta_l > \pi/2 \end{cases} \tag{5a}$$

with

$$\Phi_u = a\cos(-\cot(\theta)/\tan(\theta_l)). \tag{5b}$$

The leaf dispersion parameter $\lambda(\theta)$ equals 1 if leaves are randomly distributed, but is less than 1 for clumped canopies (e.g., Ross, 1975; Baldocchi & Collineau, 1994; España, Baret, Chelle, Aries, & Andrieu, 1998; Kucharik, Norman, & Gower, 1999; Nilson, 1971; Nouvellon et al., 2000), as in our study site. It may be expressed following (Kuusk, 1995) as

$$\lambda(\theta) = 1 - (1-\lambda_z)\frac{1-\exp[-a\tan(\theta)]}{a\tan(\theta)}, \tag{6}$$

where λ_z is the dispersion parameter in the vertical direction ($\lambda_z = \lambda(0)$), and a is a canopy structure dependent parameter (Kuusk, 1995; Kuusk, Andrieu, Chelle, & Aries, 1997).

The second model (hereafter called Mod2) is a simple and widely used model. It computes the directional radiance in terms of soil and vegetation temperatures (T_s,T_v) and emissivities (ε_s,ε_v), incoming long-wave radiation and the gap frequency function

$$R(\theta) = b(\theta)\varepsilon_s B(T_s) + [1-b(\theta)]\varepsilon_v B(T_v) + [1-\varepsilon_c(\theta)]\mathrm{Ra}, \tag{7}$$

where $\varepsilon_c(\theta)$ represents an average or effective canopy directional emissivity, which was computed here as the

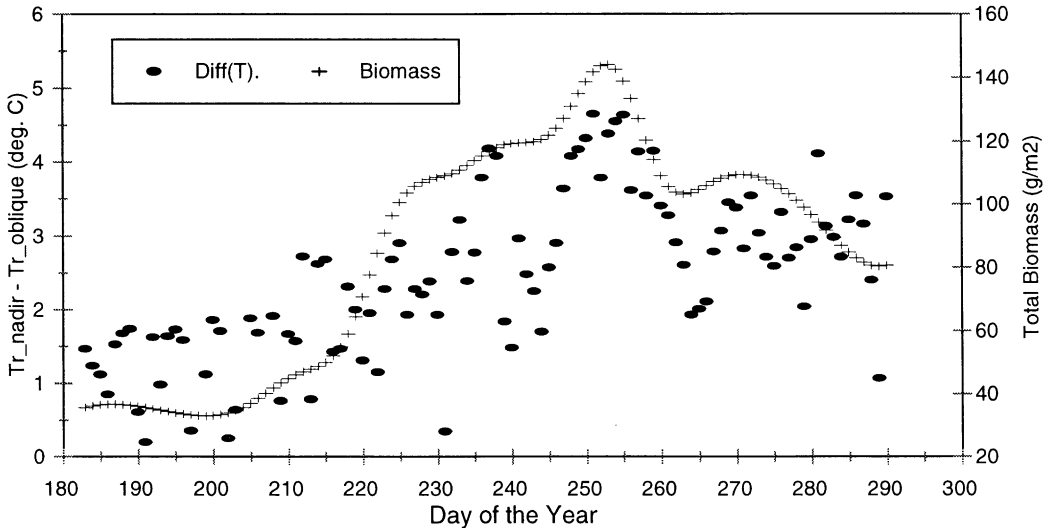

Fig. 1. Temporal variations of nadir (0°) and off-nadir (45°) temperature differences at midday along with the variation of total biomass during the 1999 growing season.

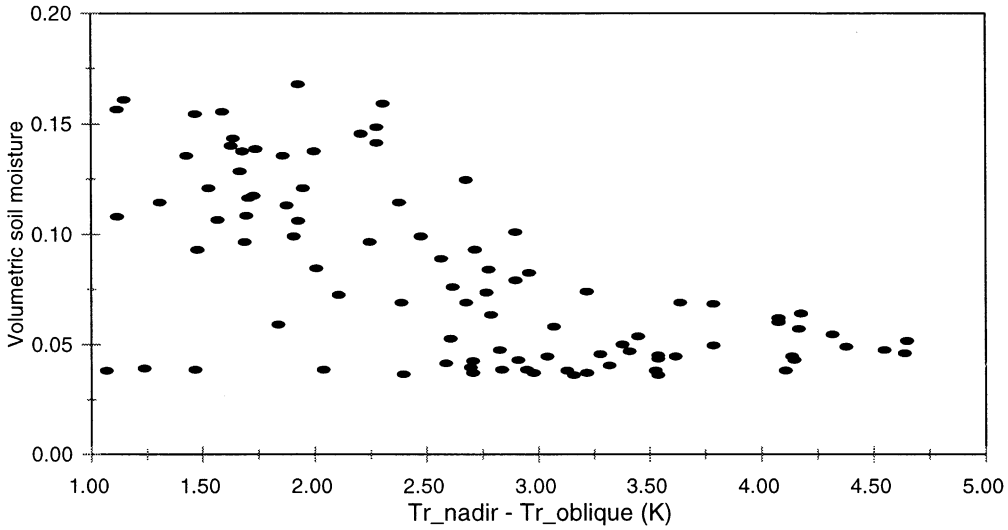

Fig. 2. Cross-plot of temperature differences and volumetric soil water content measured at 5 cm depth during the 1999 growing season.

average of soil and vegetation emissivities weighted by the directional gap frequency as:

$$\varepsilon_c(\theta) = b(\theta)\varepsilon_s + [1 - b(\theta)]\varepsilon_v. \quad (8)$$

3. Site and data description

The study site was located near the Mexican village of Zapata (110°09′W; 31°01′N; elevation 1460 m) and lies within the upper San Pedro river basin, which was the focus for SALSA activities in Mexico from 1997 to 1999 (Chehbouni et al., 2000; Goodrich et al., 2000). The natural vegetation is composed mainly of perennial grasses, the dominant species being *Bouteloua* spp. and *Eragrostis* spp.; the soil is mainly sandy loam (67% sand and 12% clay). The climate is semiarid with hot summers and cold winters and the mean annual rainfall is 440 mm.

Only data relevant to this study are presented in this section and readers are encouraged to refer to Goodrich et al. (2000) for more detail. In 1999, three 8–14 μm, infrared thermometers (IRTs, Everest International, Model 4000) were deployed at the Zapata study site, two with a

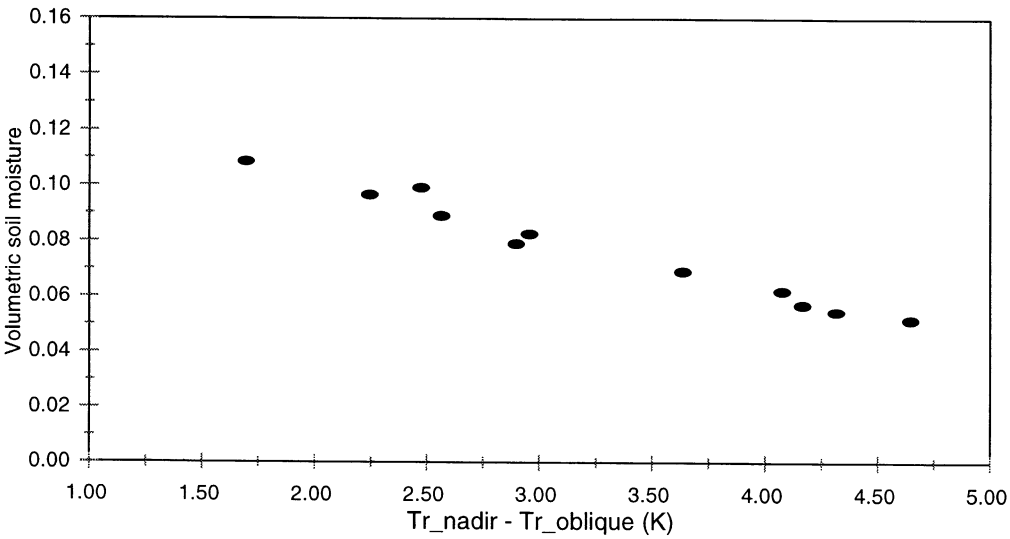

Fig. 3. Cross-plot of temperature differences and volumetric soil water content under constant vegetation conditions.

15° (±7.5) and one with a 60° (±30) field of view (FOV). Both 15° IRTs were installed on a 6-m tower, one at a height of 4.9 m aiming at an angle of 45° and the other one at a height of 3.3 m aiming at an angle of 55°. Both IRTs were oriented toward the south and pointed at the same spot. The 60° FOV IRT was installed at a height of 2.3 m, at a distance of 4.9 m from the tower and aiming vertically at the same representative spot. The height of the instruments was computed so that, given their FOVs, they sampled the same surface (i.e., there was maximum overlap between the ground FOV of each IRT). It should be mentioned that the three instruments were intercalibrated prior to the experiment. To verify the possible drift of the instrument, additional calibration was performed during the experiment by comparing their readings to a portable black body. The idea behind this particular configuration was to use two observations of directional radiative temperature to invert for component surface temperatures (i.e., soil and vegetation), and use them to simulate observations at the third angle. This configuration presents the advantage of avoiding the difficult task of accurately measuring vegetation temperature and a mean shaded–illuminated soil temperature, for a short and sparse canopy.

Green and senescent components of the biomass were monitored during the entire growing season from day of year (DOY) 180 to 295. The PAI was determined from biomass and plant specific area (PSA) measurements. Its value ranged from 0.2 to 1.1. Soil moisture was measured using time domain reflectometry (TDR) sensors (Campbell Scientific CS615 reflectometer) at different depths (5, 10, 20, 30 and 40 cm). The four components of net radiation were measured using a CNR1 (Kipp and Zonen) radiometer.

4. Results and sensitivity analysis

4.1. Examination of view-angle effect on radiative surface temperature data

In this subsection, we discuss the dependence of nadir/off-nadir radiative temperature differences on surface conditions. Differences between radiative surface temperature at nadir and at 45° at midday (1200 L.T.) along with the variation of the total biomass (green and senescent) from DOY 183 to 290 during the 1999 growing season are presented (Fig. 1). There is a general trend between the temporal variation of the temperature differences and the biomass. The maximum departure of nadir from off-nadir surface temperature (about 5 K) occurred when the biomass reached its maximum. This corresponded to a maximum contrast between dry soil and transpiring vegetation. A cross-plot between these differences and measured surface volumetric soil moisture (made at 5 cm depth) is presented in Fig. 2. The difference in temperatures generally increased with decreasing surface soil moisture. However, the relationship between soil moisture and the difference in temperatures is not a one-to-one relationship, but seems to depend also on vegetation status. For example, for a surface soil moisture of 0.04, the difference in temperatures varied between 1 and 4.5

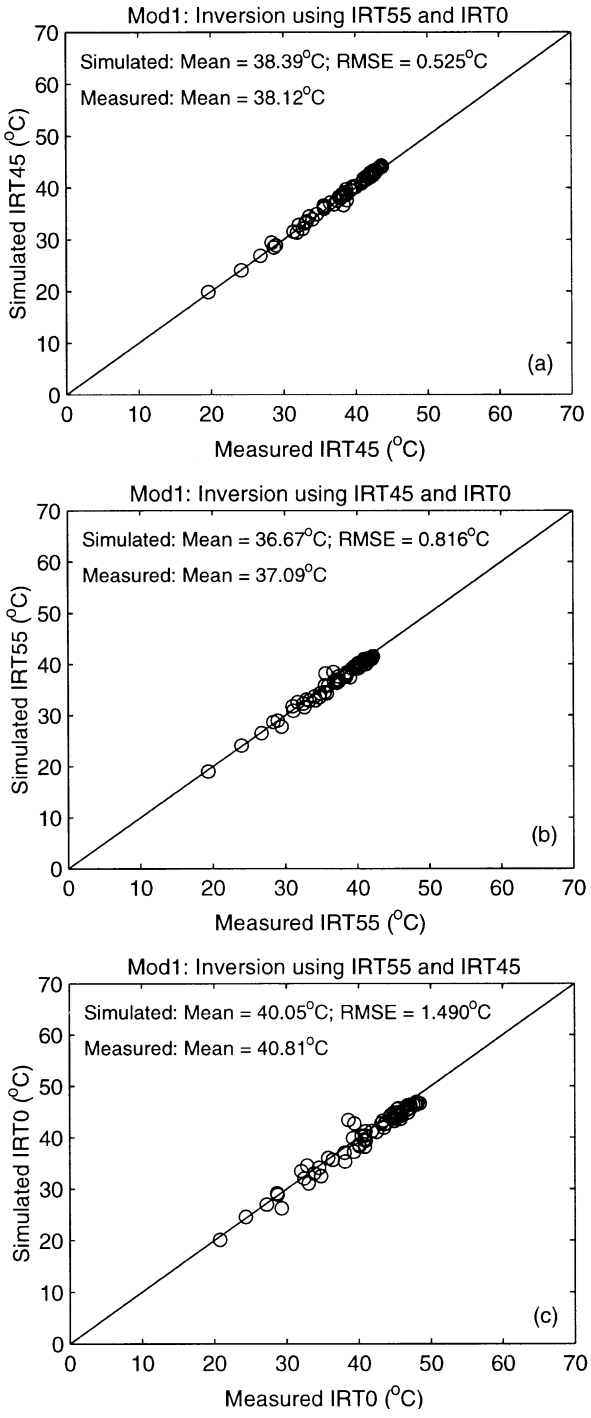

Fig. 4. Comparison between measured and Mod1-based simulations of directional radiative temperature: (a) at 45° using component temperatures inverted using observations at 0° and 55°; (b) at 55° using components temperature inverted using observations at 0° and 45°; (c) at 0° using components temperature inverted using observations at 45° and 55°.

K, depending on the PAI value. For DOY 240 to 250, which corresponds to a period where the PAI reached its maximum of 1.1 and remained unchanged, the correspondence between the temperature differences and surface soil moisture greatly improved (Fig. 3). This can be explained by the fact that under constant vegetation condition, the difference between nadir and oblique radiative temperatures increases with increasing contrast between temperature of the surface components (soil and vegetation). As can be expected, under sparsely vegetated surfaces, the difference between

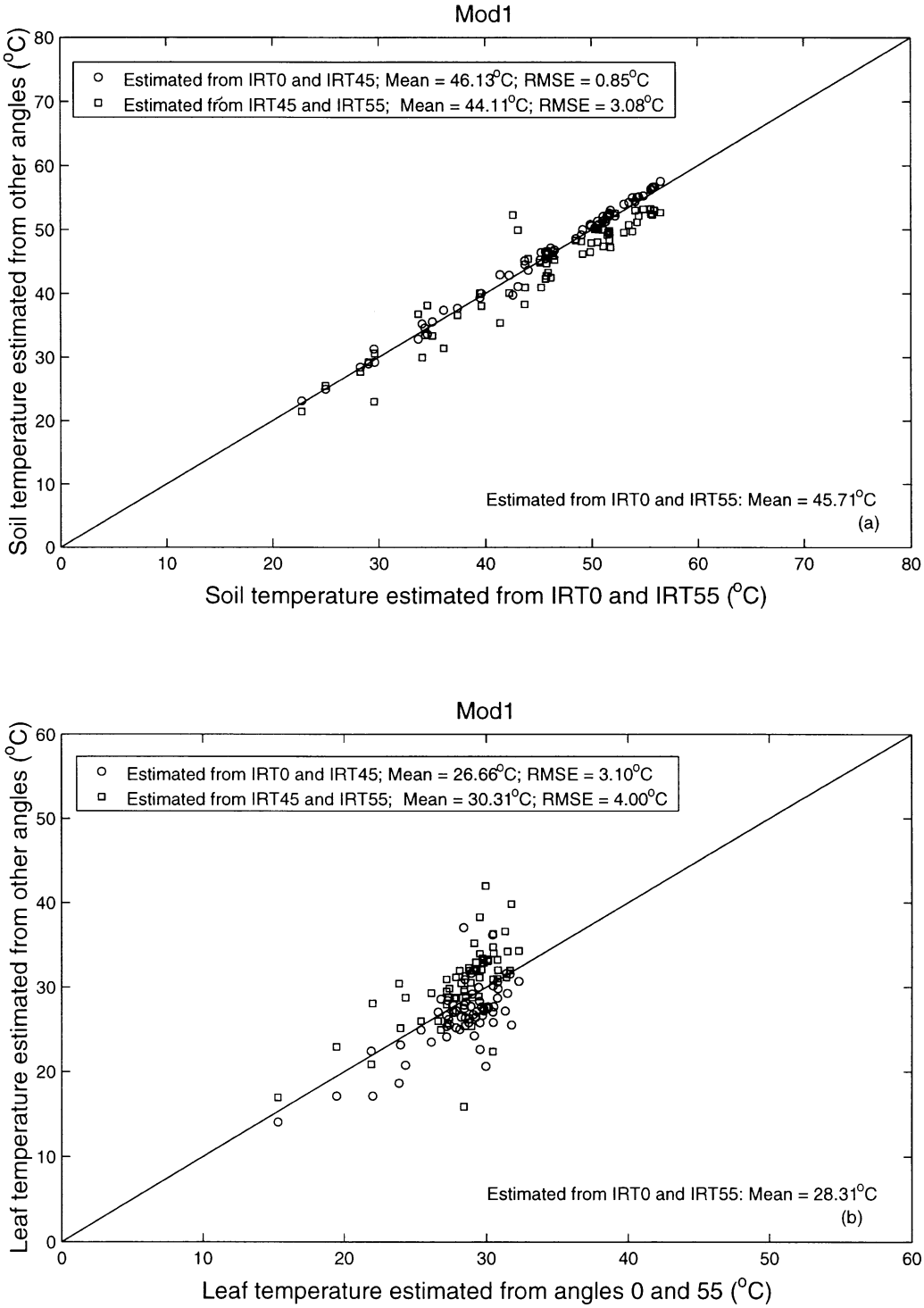

Fig. 5. Cross-plot between Mod1-based simulation of soil (a) and vegetation (b) temperatures inverted using observations at 0° and 55° and that using 0° and 55°, and 45° and 55°.

soil and vegetation temperatures was directly related to surface soil moisture. One may suggest that this relationship should also depend on wind speed, incoming solar radiation. However, since radiative surface temperature is the result of the surface equilibrium (i.e., it is not a state variable), the dependence on such variables is implicit. Therefore, under constant vegetation condition, it is possible to derive surface soil moisture from multidirectional surface temperature data. This is of interest since sensors such as ATSR can provide such directional data. However, additional investigations are needed before one can draw a firm conclusion about the robustness of this approach. Furthermore, the complementarity with a radar-based approach (Moran et al., 2000) also needs to be assessed.

4.2. Inversion results and sensitivity analysis

Both Mod1 and Mod2 have been used to invert component temperatures (soil and vegetation) from dual-angle directional temperature observations, using values of soil and vegetation emissivity, and the computed directional gap frequencies. The canopy structure parameters, including the two parameters of beta distribution (Goel & Strebel, 1984) used for the LSIDF, and the two parameters involved in the parameterization of the angular dependence of the leaf dispersion parameter (Eq. (6)) were those estimated by Nouvellon et al. (2000) on the same grasslands. The values of soil and vegetation emissivity used in this study were 0.94 and 0.98, respectively. These values are similar to those reported following an experimental investigation performed by Humes et al. (1994) in the same basin. It is worthwhile to mention that the inversion of Mod2 was achieved analytically, while that of Mod1 has to be performed numerically. In this latter case, leaf and soil temperature were estimated using an iterative procedure based on the simplex method (Nelder & Mead, 1965) that minimized the cost function E_R defined as (Eq. (9))

$$E_R = [R_{\mathrm{sim}}(\theta_1) - R_{\mathrm{obs}}(\theta_1)]^2 + [R_{\mathrm{sim}}(\theta_2) - R_{\mathrm{obs}}(\theta_2)]^2, \quad (9)$$

where $R_{\mathrm{sim}}(\theta_1)$ and $R_{\mathrm{obs}}(\theta_1)$ are the simulated and observed radiances at the first angle, and $R_{\mathrm{sim}}(\theta_2)$ and $R_{\mathrm{obs}}(\theta_2)$ are the simulated and observed radiances at the second angle. Observed directional radiances are simply derived from directional brightness temperature, where (Eq. (10))

$$R_{\mathrm{obs}}(\theta) = \sigma[T_{\mathrm{b}}(\theta)]^4. \quad (10)$$

In the case of Mod2, an analytical solution exists for inverting T_{v} and T_{s}, derived from Eq. (7), expressed at two different angles, θ_1 and θ_2, with $\theta_1 > \theta_2$, where

$$T_{\mathrm{s}} = \left\{ \frac{[1-b(\theta_1)]\sigma[T_{\mathrm{b}}(\theta_2)]^4 - [1-\varepsilon_{\mathrm{c}}(\theta_2)]\mathrm{Ra} - [1-b(\theta_2)]\sigma[T_{\mathrm{b}}(\theta_1)]^4 - [1-\varepsilon_{\mathrm{c}}(\theta_1)]\mathrm{Ra}}{\sigma\varepsilon_{\mathrm{s}}[b(\theta_2)-b(\theta_1)]} \right\}^{0.25}, \quad (11)$$

and

$$T_{\mathrm{v}} = \left\{ \frac{\sigma[T_{\mathrm{b}}(\theta_1)]^4 - [1-\varepsilon_{\mathrm{c}}(\theta_1)]\mathrm{Ra} - b(\theta_1)\varepsilon_{\mathrm{s}}\sigma T_{\mathrm{s}}^4}{\varepsilon_{\mathrm{v}}\sigma[1-b(\theta_1)]} \right\}^{0.25}. \quad (12)$$

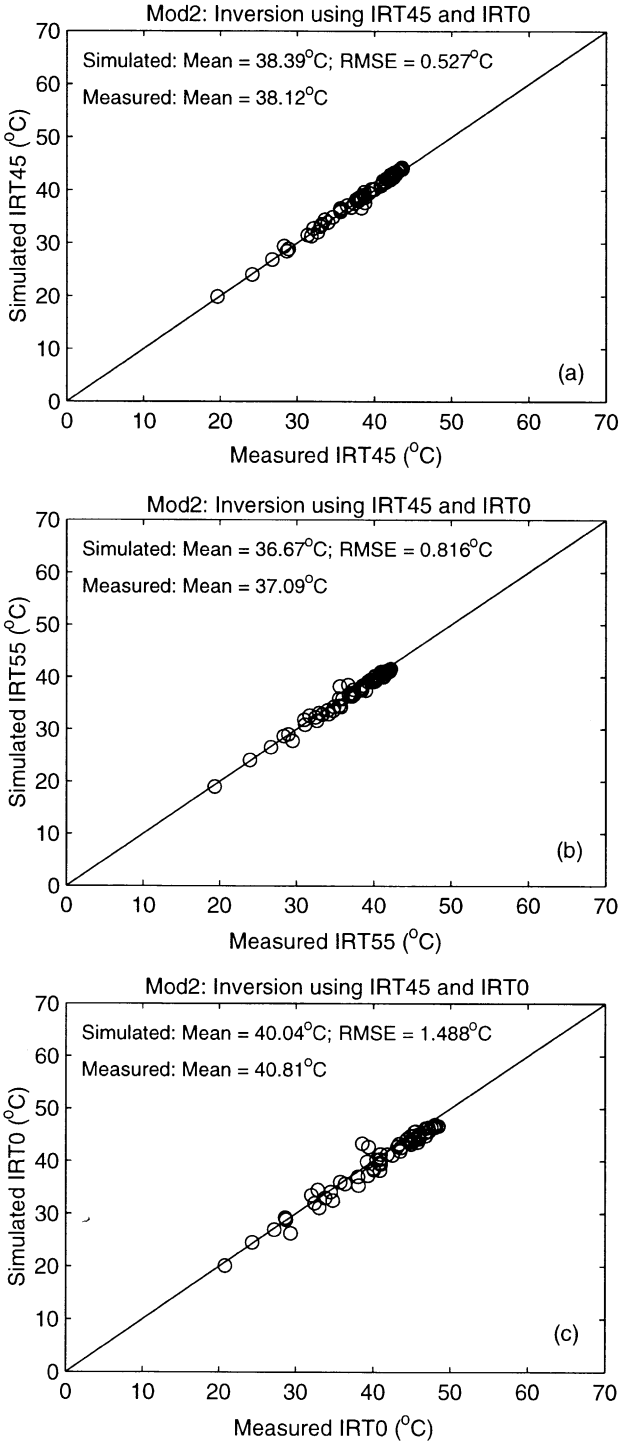

Fig. 6. Comparison between measured and Mod2-based simulations of directional radiative temperature: (a) at 45° using component temperatures inverted using observations at 0° and 55°; (b) at 55° using components temperature inverted using observations at 0° and 45°; (c) at 0° using components temperature inverted using observations at 45° and 55°.

As stated previously, the performance of the models was assessed by comparing the directional temperature observed at a third angle, with that simulated using component temperature obtained by inverting the model using two other angles. A comparison between measured directional surface temperature at 45° and that simulated by Mod1 using T_s and T_v inverted from observations at 0° and 55°, at 1200 L.T. from DOY 112 to 290 is presented in Fig. 4a. Mod1 was able to accurately reproduce the observed temperature. The root mean square error (RMSE) between

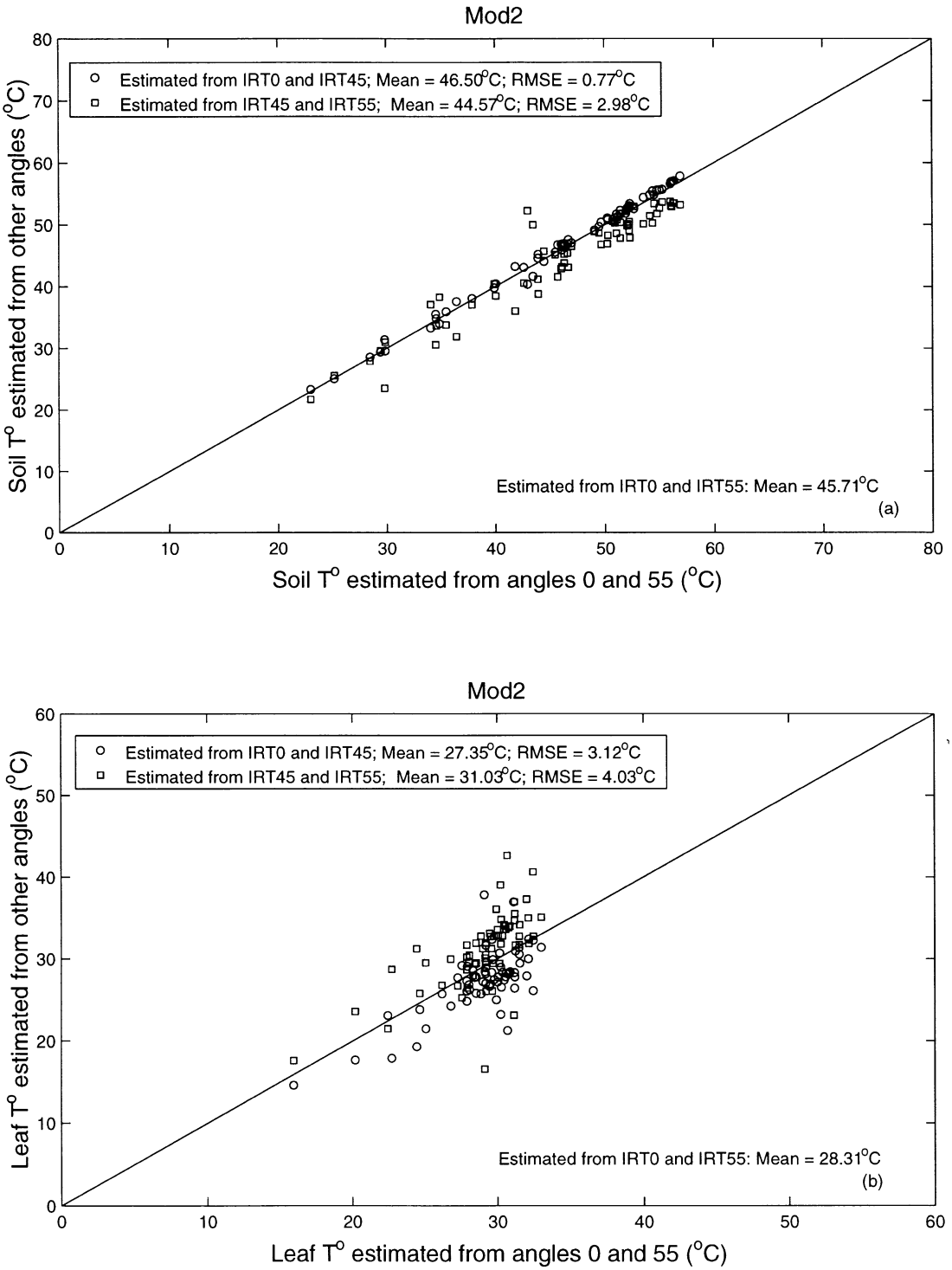

Fig. 7. Cross-plot between Mod2-based simulation of soil (a) and vegetation (b) temperatures inverted using observations at 0° and 55° and that using 0° and 55°, and 45° and 55°.

measured and simulated temperature is about 0.525 K, which is less than the expected experimental error. The same comparison as above, but using observations at other angular configuration (namely 0° and 45°, and 45° and 55°) is shown in Fig. 4b and c, respectively. Whatever the angular combination used, the model simulation is still robust. However, the accuracy of the model prediction decreases when the difference between the angles used in the inversion decreases. In this regard, the RMSE between observed and simulated directional temperature increases to a value of 1.49 K (0.816) when observation at 45° and 55° (0° and 45°) were used for the inversion. Similar findings were reported in Francois et al. (1997). This behavior can be explained by the fact that when the difference in observation angle decreased, the difference in directional temperature also decreased, which led to a larger impact of experimental errors. To investigate the effect of the choice of observation angles on inverted soil and vegetation temperatures, a cross-plot between soil temperature, inverted using 0° and 55° and those using 0° and 45°, and 45° and 55°, is presented in Fig. 5a. A similar comparison is presented in Fig. 5b for vegetation temperature. The choice of observation angles has a greater impact on the component temperatures than on the directional radiative temperature. The use of 45° and 55° observations led to an RMSE of about 3.0 K for soil temperature, which is about the double of that obtained for simulated directional temperature, using the same angular configuration. Similarly, the RMSE associated with the vegetation temperature is about 4.0 K.

Similar comparisons were performed using Mod2 (Figs. 6 and 7). The results are (perhaps surprisingly) very similar. Despite its simplicity, Mod2 seems to perform as well as the physically based, more complex Mod1. To investigate the reasons of such behavior, we adopt a heuristic approach that consists of formulating the directional radiance as

$$R(\theta) = b(\theta)\varepsilon_s B(T_s) + [1 - b(\theta)]\varepsilon_v B(T_v) + [1 - \varepsilon_c(\theta)]\mathrm{Ra} + R_{cav}(\theta), \quad (13)$$

where $\varepsilon_c(\theta)$ is the directional canopy emissivity (Eq. (8)), $R_{cav}(\theta)$ is an additional term to account for the soil–vegetation coupling or the volume scattering of the canopy, which is the base of the so-called cavity effect (Colton, 1996; Sutherland & Bartolic, 1977). The contribution of radiation interactions within the canopy cavities (or rough surfaces in general) makes the effective surface emissivity higher than that given by Eq. (8). Using a similar approach, and omitting the atmospheric contribution, Francois et al. (1997) developed a parameterization for the $R_{cav}(\theta)$ term as function of the structural parameters of the vegetation, and the radiance of the vegetation. In this study, however, this parameterization has not been used because it omits the sky contribution and it was calibrated for a different vegetation type. Instead, we directly obtained the values $R_{cav}(\theta)$ by matching the directional radiance simulated by Mod1 and that expressed using Eq. (13). The result shows that the value of $R_{cav}(\theta)$ is very small compared to the total canopy radiance. Its value ranged from 3.2 W m^{-2} for nadir view angle to 3.5 W m^{-2} for 55° view angle, which is equivalent to about 0.5 K (Table 1). Similar findings have been reported in Colton (1996). However, our results contrast with those of Francois et al. (1997), where they reported an error of about 2.4 to 3 K if the cavity effect was neglected. This can be explained by the fact that the increase in the emission term, due to lower canopy emissivity associated with ignoring the cavity effect contribution, is partially compensated by an increase in the reflection term (atmospheric radiation reflected by the canopy).

To evaluate the impact of the cavity affect term on component temperature values, we used Eq. (13) expressed at two angles (0° and 55° here) to derive soil and vegetation temperatures analytically as (Eqs. (14) and (15)):

$$T_s = \left\{ \frac{[1 - b(\theta_1)]\sigma[T_b(\theta_2)]^4 - [1 - \varepsilon_c(\theta_2)]\mathrm{Ra} - R_{cav}(\theta_2) - [1 - b(\theta_2)]\sigma[T_b(\theta_1)]^4 - [1 - \varepsilon_c(\theta_1)]\mathrm{Ra} - R_{cav}(\theta_1)}{\sigma\varepsilon_s[b(\theta_2) - b(\theta_1)]} \right\}^{0.25} \quad (14)$$

and

$$T_v = \left\{ \frac{\sigma[T_b(\theta_1)]^4 - [1 - \varepsilon_c(\theta_1)]\mathrm{Ra} - R_{cav}(\theta_1) - b(\theta_1)\varepsilon_s\sigma T_s^4}{\varepsilon_v\sigma[1 - b(\theta_1)]} \right\}^{0.25}. \quad (15)$$

The mean values of T_s and T_v estimated from these equations are about 0.41 and 0.69 K lower than those estimated from Eqs. (11) and (12). Therefore, when the cavity effect was not accounted for, vegetation and soil

Table 1
Average values of the radiance simulated with Mod1 and Mod2, the cavity effect term and the combined cavity effect–atmospheric radiation term as well as their equivalent temperature for different view angles

View zenith angle	$R(\theta)$ (Mod1) (W m^{-2})	R(θ) (Mod2) (W m^{-2})	$R_{cav}(\theta)$ (W m^{-2})	Equivalent ΔT of $R_{cav}(\theta)$ (K)	$R_{eff}(\theta)$ (W m^{-2})	Equivalent ΔT of $R_{eff}(\theta)$ (K)
0°	552.20	549.02	3.18	−0.45	21.94	−3.17
45°	534.94	531.55	3.39	−0.49	19.85	−2.93
55°	525.91	522.41	3.50	−0.52	18.74	−2.80

temperatures were overestimated, but this overestimation was not large. Consequently, it can be stated that, at least under similar conditions, the cavity effect can be safely neglected. To investigate these differences, we defined an effective term that combines both the atmospheric and cavity effects ($R_{\mathrm{eff}}'(\theta) = R_{\mathrm{cav}}(\theta) + (1 - \varepsilon_c(\theta))\mathrm{Ra}$) and we performed the same matching approach reported above. The results showed that the values of this effective term ranged from 21.9 W m^{-2} at nadir to 19.85 and 18.7 W m^{-2} at 45° and 55°, respectively (Table 1). Therefore, omitting this effective term resulted in an error of about 3 K in directional temperature. Since several authors (Choudhury et al., 1986; Lhomme et al., 1994, among others) have neglected this term in their studies, it is of interest to investigate the impact of such an assumption on the estimation of the surface sensible heat flux. We used the standard Shuttleworth and Wallace (1985) two-layer model in conjunction with typical meteorological data observed at our study site. The results show that an error of 3 K in directional radiative temperature translates to an error of about 60% in the sensible heat flux (100 W m^{-2} over our site).

A sensitivity analysis was performed to assess the impact on retrieved component temperatures of uncertainties in the values of input parameters such as soil and vegetation emissivities, PAI and error associated with directional temperature measurements. Similar to Francois et al. (1997), a set of simulations were performed with uncertainties of ±1% for emissivity, ±10 and ±20% for PAI and ±1 and ±2 K for directional temperatures. The results, presented in Table 2, indicate that the impact of uncertainties in the emissivity values is not very important. The maximum error does not exceed 0.4% in both soil and vegetation temperatures. The effect of error on PAI seemed to be much larger for the retrieved vegetation temperature than for the soil one. An error of 20% in PAI leads to an error of about 10% for vegetation temperature and of 0.34% for soil. Uncertainties in directional radiative temperature measurements appeared to have an important impact on the retrieved component temperatures. For example, an error of ±2 K leads to 7.1% (4.5%) error in retrieved vegetation (soil) temperature.

Table 2
Sensitivity of the retrieved components temperature on errors in soil and vegetation emissivities, PAI and directional radiative temperature

Variable	Variable in (%)	Absolute variation	T_v (K)	T_v (%)	T_s (K)	T_s (%)
ε_v	−1.06	−0.01	0.01	0.02	0.24	0.53
ε_s	+1.06	+0.01	0.00	0.00	−0.24	−0.52
ε_v	−1.02	−0.01	0.10	0.37	−0.01	−0.01
ε_v	+1.02	+0.01	−0.10	−0.34	0.01	0.01
PAI	−10	n.a.	−1.20	−4.23	−0.07	−0.14
PAI	+10	n.a.	0.97	3.43	0.07	0.16
PAI	−20	n.a.	−2.73	−9.63	−0.13	−0.27
PAI	+20	n.a.	1.76	6.23	0.15	0.34
IRT	−2.57	−1 K	−1.01	−3.56	−1.03	−2.24
IRT	+2.57	+1 K	1.00	3.54	1.03	2.26
IRT	−5.14	−2 K	−2.02	−7.14	−2.05	−4.49
IRT	+5.14	+2 K	2.02	7.14	2.05	4.49

5. Discussion and concluding remarks

Directional effects on thermal infrared observations have not received as much attention as have those in the optical region, despite experimental and theoretical evidence showing the importance of such effects. In this study, we first investigated the effect of view-angle variation on directional radiative temperature measurements. The experimental data showed that the differences between nadir and off-nadir values of directional temperature are of considerable magnitude and therefore cannot be ignored. The data show that this difference is controlled by several factors. The most important are vegetation and soil moisture status and conditions. The experimental data also indicated that, under sparse and constant vegetation conditions, the difference between nadir and off-nadir temperatures is well correlated to surface soil moisture. This can be explained by the fact that due to high atmospheric demand in arid and semiarid regions, the soil surface dries rapidly after a rainfall event, leading to a rapid increase in soil surface temperature. In contrast, the depletion of the root zone soil moisture and the resulting increase of vegetation temperature occur much more slowly. As a result, the increasing differences between soil and vegetation temperatures lead to increases in the difference between nadir and off-nadir radiative temperatures.

If experimentally confirmed for different vegetation types, this result is very important since it may provide a direct approach for monitoring soil moisture using remote sensing data (e.g., ATSR) at different space–time scales. However, additional studies are needed before any firm conclusions can be drawn about the feasibility and the robustness of this approach. Future work will document this finding using a hydro-ecological model coupled to a thermal infrared transfer radiative model (Cayrol et al., 1997). This will allow us to simulate the directional radiative temperature under a wide range of soil and vegetation conditions.

In this study, two radiative transfer models with different degrees of complexity were used to investigate the possibility of obtaining soil and vegetation temperatures from dual-angle measurements of directional radiative temperature. The strategy for assessing their relative performance was to use measurements at two angles to invert for soil and vegetation temperatures and then use them to simulate observations at a third angle. It might be argued that the validation cannot be fully performed since there are no

observations of component temperatures. However, it is important to keep in mind the difficulty of obtaining accurate measurements of vegetation temperature for short grass and sparse vegetation. Even slight changes in wind speed or direction may greatly affect the measurements. Similarly, it is also difficult to obtain an accurate mean (shaded–illuminated) measurement of soil temperature under such conditions. We believe that the performance of the models can be adequately assessed by comparing simulated and observed values for directional radiative temperature at a third angle and the outgoing long-wave radiation.

Despite their differences, the two models performed similarly with respect to both inverting component temperatures and simulating the third angle observations. To understand this behavior, we expressed the difference of the directional radiative surface temperature simulated by the two models as a term involving explicitly the contribution of the so-called cavity effect to the directional surface radiance. The results showed that this term was very small, and its impact on the inverted soil and vegetation temperature was not significant (0.41 and 0.69 K, respectively). Based on these results, one can conclude that — at least over this site — ignoring the cavity effect on directional radiative temperature has a smaller impact on the retrieved component temperatures than ignoring the atmospheric contribution.

A sensitivity analysis was performed to assess the effects of uncertainties of input parameters on directional and component surface temperatures. The results showed that the accuracy of the model's predictions decreased as the difference between the angles used in the inversion decreased. It also showed that an accuracy of less than 10% was required for achieving a precision of 1 K for inverted vegetation temperature. An error of 1 K in measured directional radiative temperature leads to an error of about 1 K in the inverted component temperatures. This is encouraging since the radiometric accuracy targeted with the new generation satellites is about 0.5 K or less.

The possibility of deriving component surface temperatures from dual-angle observations of directional radiative temperature, demonstrated here, presents an important step toward quantifying surface fluxes over sparsely vegetated surfaces. Future work will use both ground-based and satellite-based dual observations of surface temperature in conjunction with a dual-source model to derive soil and vegetation contribution to heat and water fluxes (Kustas & Norman, 1997). However, one has to be aware of the fact that nadir and off-nadir observations of directional radiative temperature do not correspond to the same spatial resolution when obtained from satellite-based sensors. This may limit the potential of using dual-angle observation data from ATSR, for example, to invert for component surface temperatures over heterogeneous surfaces. Fortunately, progress is being made in understanding the effect of surface heterogeneity on observed radiative temperature measurements (Njoku et al., 1996).

Acknowledgments

Funding for this study was provided by CONACYT (project: 29340T) and IRD. Additional funding was provided by Landsat7 Science Team (NASA-S-1396-F), European Union (WARTERMED project: contract no. ICA3-CT-1999-00015), and SMOS project, SALSA-global change program (NASA grant W-18,997), and the French PNTS. Many thanks to F. Santiago, J.-C. Rodriguez and M. Jauri for their valuable help during the field experiment. We are grateful to Drs. Phil Heilman and Scot Miller from USDA-ARS and to Dr. Christophe Francois of CNRS for their helpful comments on the manuscript.

References

Baldocchi, D., & Collineau, S. (1994). The physical nature of solar radiation in heterogeneous canopies: spatial and temporal attributes. In: M. M. Cadwell, & R. W. Pearcy (Eds.), *Exploitation of environmental heterogeneity by plants* (pp. 21–71). San Diego, CA: Academic Press.

Blyth, E. M., & Dolman, A. J. (1995). The roughness length for heat of sparse vegetation. *Journal of Applied Meteorology*, *34*, 583–585.

Brutsaert, W., & Sugita, M. (1996). Sensible heat transfer parameterization for surfaces with anisothermal dense vegetation. *Journal of the Atmospheric Sciences*, *53*, 209–216.

Campbell, G. S. (1986). Extinction coefficients for radiation in plant canopies calculated using an ellipsoidal inclination angle distribution. *Agricultural and Forestry Meteorology*, *36*, 317–321.

Campbell, G. S. (1990). Derivation of an angle density function for canopies with ellipsoidal leaf angle distributions. *Agricultural and Forestry Meteorology*, *49*, 173–176.

Caselles, V., Sobrino, J. A., & Coll, C. (1992). A physical model for interpreting the land surface temperature obtained by remote sensing sensors over incomplete canopies. *Remote Sensing of the Environment*, *39*, 203–211.

Cayrol, P., Chehbouni, A., Kergoat, L., Dedieu, G., Mordelet, P., & Nouvellon, Y. (2000). Grassland modeling and monitoring with SPOT-4 vegetation instrument during the 1997–1999 SALSA experiment. *Agricultural and Forestry Meteorology, 105,* 91–115.

Chehbouni, A., Goodrich, D. C., Moran, M. S., Watts, C. J., Kerr, Y. H., Dedieu, G., Kepner, W. G., Shuttleworth, W. J., & Sorooshian, S. (2000). A preliminary synthesis of major scientific results during the SALSA program. *Agricultural and Forestry Meteorology, 105,* 311–323.

Chehbouni, A., Lo Seen, D., Njoku, E. G., Lhomme, J. P., Monteny, B., & Kerr, Y. H. (1997). Estimation of sensible heat flux over sparsely vegetated surfaces: relationship between radiative and aerodynamic surface temperature. *Journal of Hydrology*, *188–189*, 855–868.

Chehbouni, A., Lo Seen, D., Njoku, E. G., & Monteny, B. (1996). Examination of the difference between radiative and aerodynamic surface temperatures over sparsely vegetated surfaces. *Remote Sensing of the Environment*, *58*, 177–186.

Chehbouni, A., Watts, C., Kerr, Y. H., Dedieu, G., Rodriguez, J.-C., Santiago, F., Cayrol, P., Boulet, G., & Goodrich, D. (2000). Methods to aggregate turbulent fluxes over heterogeneous surfaces: application to SALSA data set in Mexico. *Agricultural and Forestry Meteorology, 105*, 133–144.

Choudhury, B. J., Reginato, R. J., & Idso, S. B. (1986). An analysis of infrared temperature observations over wheat and calculation of latent heat flux. *Agricultural and Forestry Meteorology.*, *37*, 75–88.

Colton, A. L. (1996). Effective thermal parameters for a heterogeneous land surface. *Remote Sensing of the Environment*, *57*, 143–160.

España, M., Baret, F., Chelle, M., Aries, F., & Andrieu, B. (1998). A dynamic model of maize 3D architecture: application to the parameterisation of the clumpiness of the canopy. *Agronomy Journal*, *18*, 609–626.

Francois, C., Ottle, C., & Prevot, L. (1997). Analytical parameterization of canopy directional in the thermal infrared. Application on the retrieval of soil and foliage temperatures using two directional measurements. *International Journal of Remote Sensing*, *12* (18), 2587–2621.

Goel, N. S., & Strebel, D. E. (1984). Simple beta distribution representation of leaf orientation in vegetation canopies. *Agronomy Journal*, *75*, 800–802.

Goodrich, D. C., Chehbouni, A., Goff, B., MacNish, B., Maddock, T., Moran, S., Shuttleworth, W. J., Williams, D. G., Watts, C., Hipps, L. H., Cooper, D. I., Schieldge, J., Kerr, Y. H., Arias, H., Kirkland, M., Carlos, R., Cayrol, P., Kepner, W., Jones, B., Avissar, R., Begue A., Bonnefond, J.-M., Boulet, G., Branan, B., Brunel, J. P., Chen, L. C., Clarke, T., Davis, M. R., DeBruin, H., Dedieu, G., Elguero, E., Eichinger, W. E., Everitt, J., Garatuza-Payan, J., Gempko, V. L., Gupta, H., Harlow, C., Hartogensis, O., Helfer, M., Holifield, C., Hymer, D., Kahle, A., Keefer, T., Krishnamoorthy, S., Lhomme, J.-P., Lagouarde, J-P., Lo Seen, D., Luquet, D., Marsett, R., Monteny, B., Ni, W., Nouvellon, Y., Pinker, R., Peters, C., Pool, D., Qi, J., Rambal, S., Rodriguez, J., Santiago, F., Sano, E., Schaeffer, S. M., Schulte, M., Scott, R., Shao, X., Snyder, K. A., Sorooshian, S., Unkrich, C. L., Whitaker, M., & Yucel, I. (2000). Preface paper to the Semi-Arid Land-Surface-Atmosphere(SALSA) Program special issue, *Agricultural and Forestry Meteorology, 105*, 3–20.

Hall, G. H., Huemmrich, K. F., Goetz, S. J., Sellers, P. J., & Nickeson, J. E. (1992). Satellite remote sensing of surface energy balance: success, failure and unresolved issues in FIFE. *Journal of Geophysical Research*, *97*, 19061–19089.

Heilman, J. L., Heilman, W. E., & Moore, D. G. (1981). Remote sensing of canopy temperature at incomplete cover. *Agronomy Journal*, *73*, 403–406.

Humes, K. S., Kustas, W. P., Moran, M. S., Nichols, W. D., & Weltz, M. A. (1994). Variability of emissivity and surface temperature over sparsely vegetated surface. *Water Resources Research*, *30*, 1299–1310.

Jackson, R. D., Reginato, R. J., & Idso, S. B. (1977). Wheat canopy temperature: a practical tool for evaluating water requirements. *Water Resources Management*, *13*, 651–656.

Kimes, D. S. (1980). Effect of vegetation canopy structure on remotely sensed canopy temperatures. *Remote Sensing of the Environment*, *10*, 165–174.

Kimes, D. S. (1981). Remote sensing of temperature profiles in vegetation canopies using multiple view angle and inversion techniques. *IEEE Transactions on Geoscience Remote Sensing*, *GE-19* (2), 85–90.

Kimes, D. S. (1983). Remote sensing of row crop structure and component temperatures using directional radiometric temperatures and inversion techniques. *Remote Sensing of the Environment*, *13*, 33–55.

Kubota, A., & Sugita, M. (1994). Radiometrically determined skin temperature and scalar roughness to estimate surface heat flux: Part I. Parameterization of radiometric scalar roughness. *Boundary-Layer Meteorology*, *69*, 397–416.

Kucharik, C. J., Norman, J. M., & Gower, S. T. (1999). Characterization of radiation regimes in nonrandom forest canopies: theory, measurements, and a simplified modeling approach. *Tree Physiology*, *19*, 695–706.

Kustas, W. P., Choudhury, B. J., Inoue, Y., Pinter, P. J., Moran, M. S., Jackson, R. D., & Reginato, R. J. (1990). Ground and aircraft infrared observations over a partially vegetated area. *International Journal of Remote Sensing*, *3*, 409–428.

Kustas, W. P., Choudhury, B. J., Moran, M. S., Reginato, R. J., Jackson, R. D., Gay, L. W., & Weaver, H. L. (1989). Determination of sensible heat flux over sparse canopy using thermal infrared data. *Agricultural and Forestry Meteorology*, *44*, 197–216.

Kustas, W. P., & Norman, J. M. (1997). A two-source approach for estimating turbulent fluxes using multiple angle thermal infrared observations. *Water Resources Research*, *33*, 1495–1508.

Kuusk, A. (1995). A Markov chain model of canopy reflectance. *Agricultural and Forestry Meteorology*, *76*, 221–236.

Kuusk, A., Andrieu, B., Chelle, M., & Aries, F. (1997). Validation of a Markov chain canopy reflectance model. *International Journal of Remote Sensing*, *18* (10), 2125–2146.

Lagouarde, J. P., Ballans, H., Moreau, P., Guyon, D., & Caraboeuf, D. (2000). Experimental study of brightness surface temperature angular variations of maritime pine (*Pinus pinaster*) stands. *Remote Sensing of the Environment*, *72*, 17–34.

Lagouarde, J. P., Kerr, Y. H., & Brunet, Y. (1995). An experimental study of angular effects on surface temperature for various plant canopies and bare soils. *Agricultural and Forestry Meteorology*, *77*, 167–190.

Lhomme, J. P., Monteny, B., Chehbouni, A., & Troufleau, D. (1994). Determination of sensible heat flux over Sahelian fallow savannah using infra-red thermometry. *Agricultural and Forestry Meteorology.*, *68*, 93–105.

Lhomme, J.-P., Monteny, B., Troufleau, D., Chehbouni, A., & Bauduin, S. (1997). Sensible heat flux and radiometric surface temperature over sparse sahelian vegetation: a model for the kB^{-1} parameter. *Journal of Hydrology*, *189*, 839–854.

Mathias, A. D., Yates, S. R., Zhang, R., & Warrick, A. W. (1987). Radiant temperatures of sparse plant canopies and soil using IR thermometry. *IEEE Transactions on Geoscience Remote Sensing*, *25*, 516–519.

McGuire, M. J., Balick, L. G., Smith, J. A., & Hutchison, B. A. (1989). Modeling directional thermal radiance from a forest canopy. *Remote Sensing of the Environment*, *27*, 169–186.

Moran, M. S., Humes, K. S., & Pinter, P. J. (1997). The scaling characteristics of remotely-sensed variables for sparsely-vegetated heterogeneous landscapes. *Journal of Hydrology*, *190*, 337–362.

Moran, M. S., Hymer, D. C., Qi, J., & Sano, E. E. (2000). Soil moisture evaluation using synthetic aperture radar (SAR) and optical remote-sensing in semiarid rangeland. *Agricultural and Forestry Meteorology, 105*, 69–80.

Moran, M. S., Kustas, W. P., Vidal, A., Stannard, D. I., Blanford, J. H., & Nichols, W. D. (1994). Use of ground-based remotely sensed data for surface energy balance evaluation in a semi-arid rangeland. *Water Resources Research*, *30*, 1339–1349.

Nelder, J. A., & Mead, R. (1965). A simplex method for function minimization. *Computer Journal*, *7*, 308–313.

Nilson, T. (1971). A theoretical analysis of the frequency of gaps in plant stands. *Agriculture and Meteorology*, *8*, 25–38.

Njoku, E. G., Hook, S. J., & Chehbouni, A. (1996). Effects of surface heterogeneity on thermal remote sensing of land parameters. (Chap. 2). In: J. B. Stewart, E. T. Engman, R. A. Feddes, & Y. Kerr (Eds.), *Scaling up in hydrology using remote sensing.* (pp. 19–37). West Sussex, UK: John Wiley & sons.

Norman, J. M., & Becker, F. (1995). Terminology in thermal infrared remote sensing of natural surfaces. *Agricultural and Forestry Meteorology*, *77*, 153–166.

Nouvellon, Y. P., Bégué, A., Moran, M. S., Lo Seen, D., Rambal, S., Luquet, D., Chehbouni, A., & Inoue, Y. (2000). PAR extinction in shortgrass-ecosystems: effects of clumping, sky conditions and soil albedo. *Agricultural and Forestry Meteorology, 105,* 21–42.

Prata, A. J. (1990). Land surface temperature derived from AVHRR and ATSR I: theory. *Journal of Geophysical Research*, *98*, 16689–16702.

Prevot, L. (1985). Modelisation des echanges radiatifs au sein des couverts vegetales: application a la teledetection. Validation sur un couvert de mais. PhD dissertation, University of Paris.

Ross, J. (1975). Radiative transfer in plant communities. In: J. L. Monteith (Ed.), *Vegetation and the atmosphere* (pp. 13–55). San Diego, CA: Academic Press.

Shuttleworth, W. J., & Wallace, J. S. (1985). Evaporation from sparse crops — an energy combination theory. *Quarterly Journal of the Royal Meteorological Society*, *111*, 839–855.

Smith, J. A., & Goltz, S. M. (1994). Updated thermal model using simplified short-wave radiosity calculations. *Remote Sensing of the Environment*, *47*, 167–175.

Sobrino, J. A., & Caselles (1990). Thermal infrared radiance model for interpreting the directional radiometric temperature of a vegetative surface. *Remote Sensing of the Environment*, *33*, 193–199.

Stewart, J. B., Kustas, W. P., Humes, K. S., Nichols, W. D., Moran, M. S., & de Bruin, H. A. R. (1994). Sensible heat flux–radiometric surface temperature relationship for eight semi-arid areas. *Journal of Applied Meteorology*, *33*, 1110–1117.

Sugita, M., & Brutsaert, W. (1996). Optimal measurement strategy for surface temperature to determine sensible heat flux from anisothermal vegetation. *Water Resources Research*, *32*, 2129–2134.

Sun, J., & Mahrt, L. (1995). Determination of surface fluxes from the surface radiative temperature. *Journal of the Atmospheric Sciences*, *52*, 1096–1106.

Sutherland, R. A., & Bartolic, J. F. (1977). Significance of vegetation in interpreting thermal radiation from a terrestrial surface. *Applied Meteorology*, *16*, 759–763.

Taconet, O., Bernard, R., & Vidal-Madjar, D. (1986). Evapotranspiration over an agricultural region using a surface flux/temperature model based on NOAA-AVHRR data. *Journal of Climate and Applied Meteorology*, *25*, 284–307.

Troufleau, D., Lhomme, J.-P., Monteny, B., & Vidal, A. (1997). Sensible heat flux and radiometric surface temperature over sparse sahelian vegetation: is the kB^{-1} a relevant parameter. *Journal of Hydrology*, *189*, 815–838.

Warren, W. J. (1960). Inclined point quadrat. *New Phytologist*, *58*, 92–101.

Watts, C. J., Chehbouni, A., Rodriguez, J.-C., Kerr, Y. H., Hartogensis, O., & De Bruin, H. A. R. (2000). Comparison of sensible heat flux estimates using AVHRR with scintillometer measurements over semi-arid grassland in northwest Mexico. *Agricultural and Forestry Meteorology, 105*, 81–89.